Catena 261 (2025) 109582

Contents lists available at ScienceDirect

Catena

journal homepage: www.elsevier.com/locate/catena

Integrated physical–chemical mechanisms drive carbon stabilization under conservation tillage in Karst agroecosystems

Guang Xu[a], Qishun Mo[b], Zhou Li[a,c,*], Wangfei Qin[a], Rui Dong[a], Xuechun Zhao[a], Chao Chen[a], Anna Gunina[d], Narasinha Shurpali[e], Tulasi Lakshmi Thentu[e], Gang Nie[f], Yuan Li[e,*]

[a] Key Laboratory of Animal Genetics, Breeding and Reproduction in the Plateau Mountainous Region, Ministry of Education, College of Animal Science, Guizhou University, Guiyang 550025, China
[b] Animal Husbandry Development Centre of Tianzhu County Agriculture and Rural Bureau, Qiandongnan Miao and Dong Autonomous Prefecture, 556600, China
[c] Department of Renewable Resources, University of Alberta, Edmonton, AB T6G 2E3, Canada
[d] Ostwestfalen-Lippe University of Applied Sciences and Arts, Höxtet 37671, Germany
[e] Grassland and Sustainable Farming Production systems, Natural Resources Institute Finland, Maaninka FI-71750, Finland
[f] College of Grassland Science and Technology, Sichuan Agricultural University, Chengdu 611130, China

ARTICLE INFO

Keywords:
Aggregate stability
Carbon fractions
Conservation tillage
FTIR spectroscopy

ABSTRACT

Conservation tillage practices improve soil fertility and enhance soil organic carbon (SOC) sequestration in fragile Karst agroecosystems. In a three-year field experiment in Southwest China aimed to compare conventional tillage (CT), conventional tillage-mulching (CTM), no-tillage without mulching (NT), and no-tillage-mulching (NTM) and evaluate their effects on SOC accumulation in aggregation, changes in SOC composition and actives of C-related enzymes at depths of 0 – 5, 5 – 10, and 10 – 20 cm. Large macroaggregates (> 2 mm) dominated (54 – 64 %), and NTM increased the proportion of > 2 mm aggregates in the 0 – 5 cm. All conservation tillage practices enhanced macroaggregate stability, with NTM showing the greatest improvements in mean weight diameter and SOC content across aggregate size classes. FTIR indicated that NTM increased the intensity of carboxyl-C in macroaggregates, suggesting enhanced chemical stabilization. Soil oxidases (polyphenol oxidase, peroxidase) and hydrolases (β-1,4-glucosidase) generally increased under conservation tillage, although responses of other enzymes (e.g., cellobiohydrolase, β-xylosidase) varied by depth and aggregate size. Structural equation modeling revealed that no-tillage promoted enzyme activities (path coefficient = 0.77), while mulching improved soil aggregation (0.60) and enzyme activities (0.32), which all increased SOC content. Thus, no-tillage combined with mulching is the most effective strategy for improving aggregate stability, SOC content, and enzymatic activities in Karst agricultural systems, offering a practical approach for sustainable land management.

1. Introduction

The accelerating rise of CO_2 and the increasing frequency of extreme weather events have intensified global concerns regarding climate change and its impacts on agricultural sustainability (Lal, 2004; Ma et al., 2024; Hashimi et al., 2023; Reynaert et al., 2024; Mhlanga et al., 2022). Among the landscapes most vulnerable to these challenges are Karst regions, which cover approximately 12 % of the world's land surface (Jiang et al., 2014). These areas commonly face persistent constraints such as low soil fertility, frequent erosion due to shallow soil depth, and intensive agricultural management (Xiong et al., 2008; Zhang et al., 2019). In southwestern China, the Karst region spans approximately 55 x 10^4 km^2 (Jiang et al., 2014) and is recognized as one of the largest and most ecologically sensitive Karst terrains globally. The shallow soil depth and high infiltration rates in these landscapes can accelerate the loss of soil organic carbon (SOC), complicating efforts to maintain land productivity and stability (Liu et al., 2024; Qin et al., 2017). Thus, identifying management strategies that enhance SOC accumulation and improve soil conditions is essential for mitigating land degradation and ensuring long-term agricultural sustainability in Karst

* Corresponding authors.
E-mail addresses: zli8@gzu.edu.cn (Z. Li), yuan.li@luke.fi (Y. Li).

https://doi.org/10.1016/j.catena.2025.109582
Received 24 January 2025; Received in revised form 8 June 2025; Accepted 20 October 2025
Available online 26 October 2025

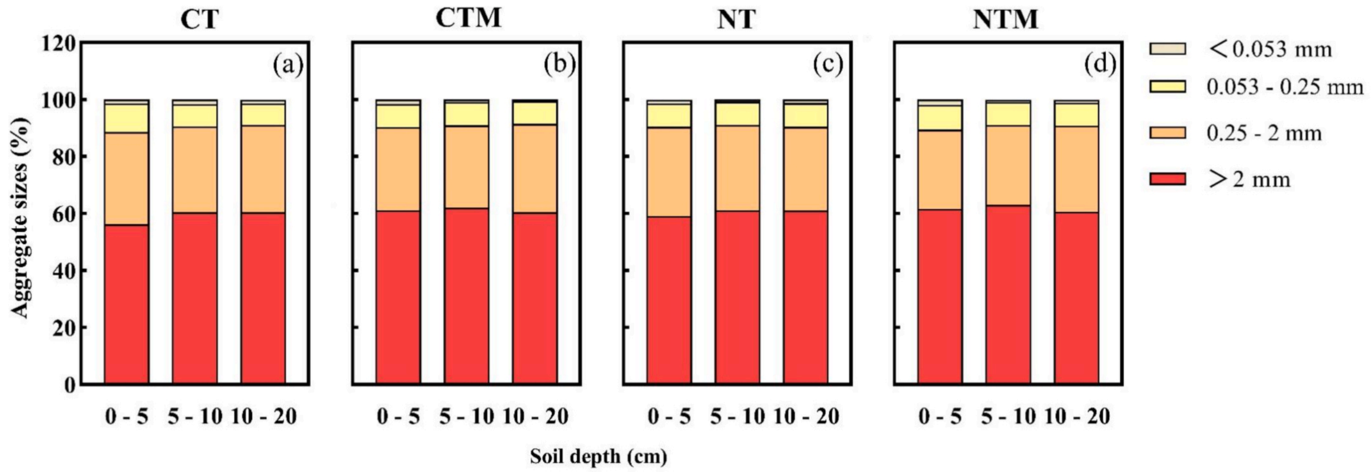

Fig. 1. Effects of conservation tillage practices on soil aggregate size distribution at different depths (0–20 cm). Values represent the percentage of each aggregate size class (> 2 mm, 0.25–2 mm, 0.053–0.25 mm, and < 0.053 mm) under different tillage treatments a) CT: conventional tillage; b) CTM: conventional tillage-mulching; c) NT: no-tillage; d) NTM: no-tillage −mulching).

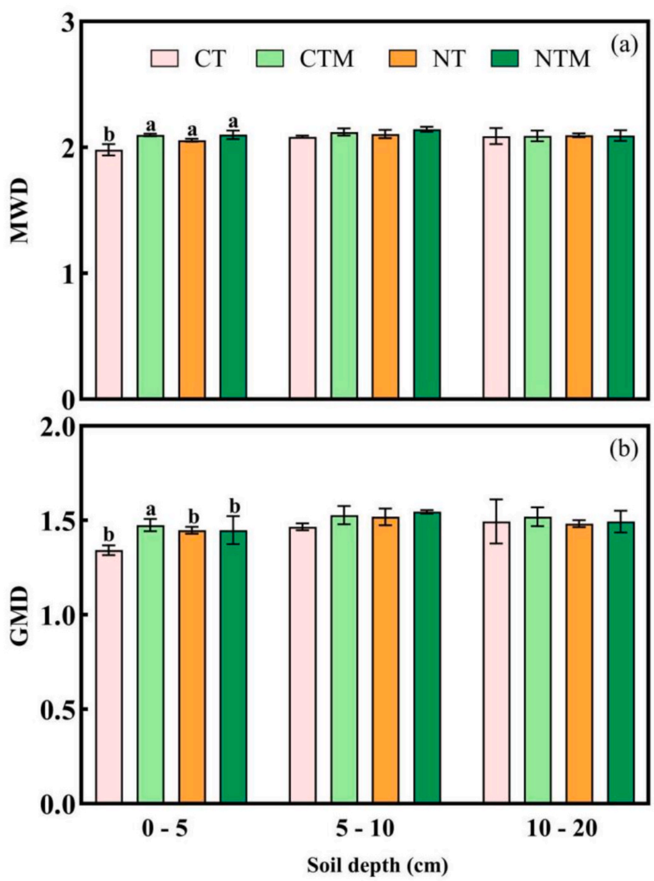

Fig. 2. Impact of conservation tillage practices on soil aggregate stability indices: a) mean weight diameter (MWD) and b) geometric mean diameter (GMD) across soil depths (0–20 cm). Letters indicate significant differences between treatments at $p < 0.05$. CT: conventional tillage; CTM: conventional tillage-mulching; NT: no-tillage; NTM: no-tillage-mulching).

regions.

Conservation tillage, particularly no-tillage combined with surface mulching, has drawn increasing attention as a strategy for improving fertility and increasing SOC storage (Li et al., 2021; Melero et al., 2009; Rocco et al., 2024; Singh et al., 2023). These practices can increase SOC sequestration by improving aggregate formation and stability and reducing erosion (Honkanen et al., 2021; Nebbioso and Piccolo, 2012; Xing et al., 2023). Previous studies have shown that hydrophobic organic compounds accumulate in large aggregates (>2000 μm), contributing to their stability, while more hydrophilic ones are associated with small aggregate fractions (Nebbioso and Piccolo, 2012). Although several studies have examined how no-tillage affects SOC sequestration within aggregates (Kan et al., 2020), studies specifically addressing these processes in soils in Karst regions remain limited, and the mechanisms driving SOC stabilization under conservation tillage in Karst regions are not fully understood.

The chemical composition of SOC, determined through analytical techniques such as Fourier transform infrared (FTIR) spectroscopy, provides valuable insights into carbon stability and turnover (Capriel, 1997; Peltre et al., 2017). Stable fractions, such as aromatic and carboxyl compounds, often resist decomposition and thus contribute to long-term SOC storage (Shao et al., 2019). Previous research has demonstrated that FTIR can detect shifts in SOC functional groups within aggregates; however, studies linking conservation tillage practices to changes in SOC chemistry and aggregate-associated stability in soils of Karst regions are limited. Moreover, even if previous work showed that no-tillage or residue retention can improve enzyme activities related to C cycling (e.g., β-1,4-glucosidase, polyphenol oxidase, peroxidase, and β-1,4-xylosidase), the relationships between enzyme activities, SOC chemical composition, and aggregate size fractions in soils in Karst regions remain poorly understood (He et al., 2021; Liu et al., 2024; Xiao et al., 2024; Qin et al., 2017; Liu et al., 2023; Zhu et al., 2024). Thus, although no-tillage and mulching are promoted for their potential to enhance SOC sequestration, research in Karst agro-ecosystems remains limited regarding how these practices jointly affect aggregate structure, SOC chemical composition, and enzymatic processes related to carbon stabilization.

Therefore, this study evaluated the influence of combinations of no-tillage and mulching on soil aggregation, SOC content, chemical composition, and carbon-related enzyme activities in a Karst agro-ecosystem, compared to conventional tillage. We hypothesized that: 1) no-tillage with mulching would promote macroaggregate formation compared to conventional tillage; 2) no-tillage and no-tillage with mulching would increase SOC content, particularly in large aggregates in topsoil compared to conventional tillage; 3) no-tillage and no-tillage with mulching would enhance more stable SOC fractions (aromatic and carboxyl groups) compared to conventional tillage; and 4) no-tillage and no-tillage with mulching would improve enzyme activities involved in C cycling compared to conventional tillage.

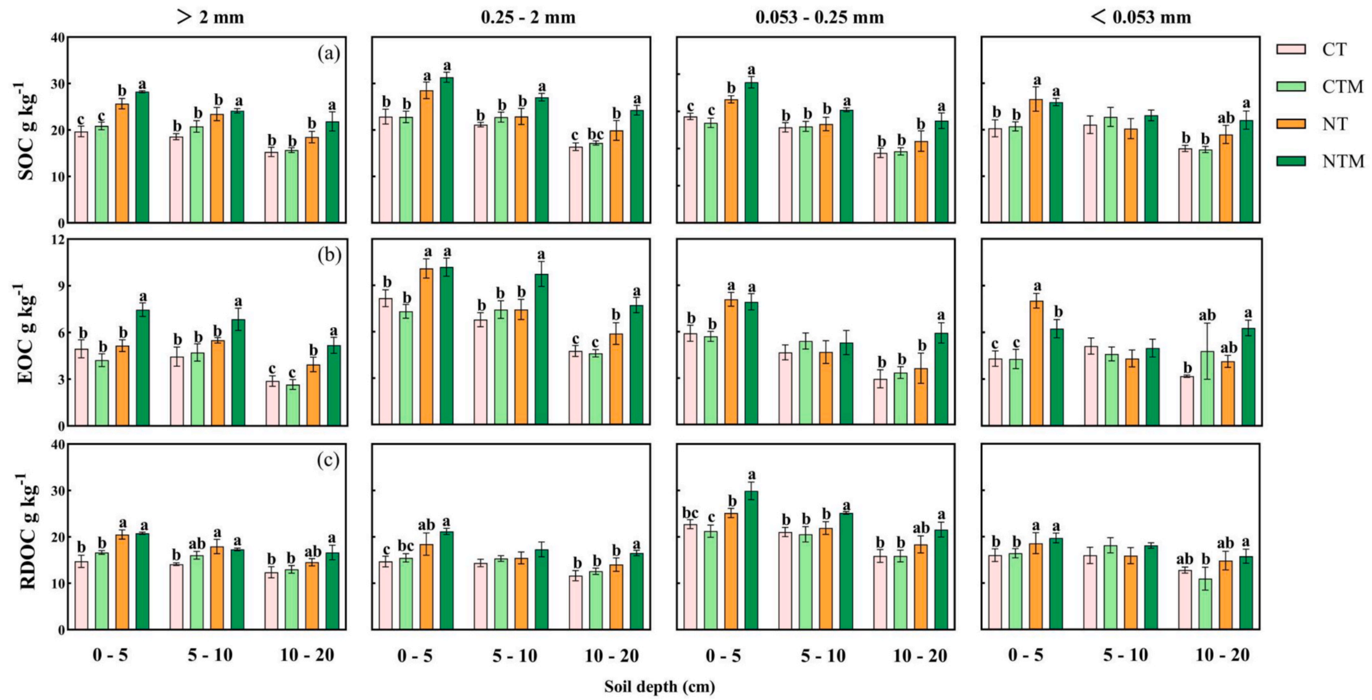

Fig. 3. Distribution of soil organic carbon fractions (total soil organic carbon, SOC; easily oxidizable organic carbon, EOC; and recalcitrant organic carbon, RDOC) within different aggregate size classes across soil depths under conservation tillage practices. Letters indicate significant differences between treatments at $p < 0.05$. CT: conventional tillage; CTM: conventional tillage-mulching; NT: no-tillage; NTM: no-tillage-mulching).

2. Materials and methods

2.1. Experimental site

The experiment was conducted at the forage rotation experimental station of Guizhou University in Dafang County, Bijie City, Guizhou Province, China (27°41′N, 105°89′E, altitude 1723 m). The area experiences a humid subtropical monsoon climate, representing typical Guizhou Karst topography and climatic conditions. The average annual rainfall is 1154 mm, and the mean temperature is approximately 11.8 °C, with extremes of 32.7 °C and −9.3 °C. According to the World Reference Base for Soil Resources (IUSS Working Group WRB, 2022) for Soil Resources, the predominant soil type in the study area is Ali-Perudic Argosols (Qin et al., 2023) (equivalent to Alfisols in the United States Department of Agriculture (USDA) Classification of Soil Systems) (United States Department of Agriculture (USDA), 1999). In 0 – 20 cm horizon, the average pH is 4.92 and the clay content is 24.6 %. From 2020 to 2023, the site was used for a forage maize (*Zea mays*) and hairy vetch (*Vicia villosa*) rotation experiment.

2.2. Experimental design

The experiment followed a completely randomized block design, with the factors of tillage (2 factor levels, conventional tillage (20 cm deep rotary tillage) and no-tillage) and cover crop (2 factor levels: cover crop mulching and no mulching (Table S1)). In total, four treatments were created: conventional tillage without cover crop mulching (conventional tillage, CT), conventional tillage with cover crop mulching (conventional tillage-mulching, CTM), and no-tillage without cover crop mulching (no-tillage, NT), no-tillage with cover crop mulching (no-tillage-mulching, NTM), each replicated three times, resulting in 12 plots. The plot size was 30.24 m^2 (7.2 m × 4.2 m), with plots separated by a 1 mm thick, 20 cm wide plastic barrier, 10 cm inserted into the soil and 10 cm aboveground to minimize cross-plot interactions.

Implementing the cover crop-maize system commenced with the establishment of the cover crop (hairy vetch, 'Lushao No. 1′). The cover crop was sown at a seeding rate of 60 kg ha^{-1} in a uniform row configuration with 20 cm inter-row and intra-row spacing. Prior to sowing, basal fertilization was implemented through the single superphosphate (12 % P_2O_5) at 75 kg ha^{-1} and potassium sulfate (60 % K_2SO_4) at 75 kg ha^{-1}. Following the subsequent maize harvest, the hairy vetch was sown immediately and killed before maize planting, covered over the soil surface, forming a continuous layer of organic mulch.

The Forage maize ('Qianqing 446′) sown in a wide-narrow row spacing pattern (80 cm and 40 cm, respectively), with a plant spacing of 20 cm, resulting in a planting density of 81,000 plants per hectare. Basal fertilization included compound fertilizer ($N:P_2O_5:K_2O$ = 15:15:15) at 225 kg ha^{-1} and superphosphate at 330 kg ha^{-1}. The first topdressing was applied at the V6 stage (approximately the sixth-leaf stage), with nitrogen fertilizer at a rate of 120 kg ha^{-1}. The second topdressing was applied at the tasseling (VT) stage, applying nitrogen fertilizer at 180 kg ha^{-1}.

Maize was sown on April 24, 2021, and harvested on September 8, 2021; in 2022, maize was planted on April 27 and harvested on September 14; in 2023, it was sown on April 27 and harvested on September 13.

2.3. Soil sampling

Soil samples were collected in September 2023 after the maize harvest. A five-point sampling method was used to collect soil samples from 0 to 5, 5 – 10, and 10 – 20 cm depths. Samples were collected from the center of each microplot and thoroughly mixed to form a composite sample. The samples were air-dried at ambient temperature (20 – 25 °C) after removing stones, gravel, and plant residues. Part of the soil was passed through a 2 mm sieve for analysis of total soil carbon and physical structure. Another part was passed through an 8 mm sieve for aggregate separation and to measure easily oxidizable organic carbon (EOC).

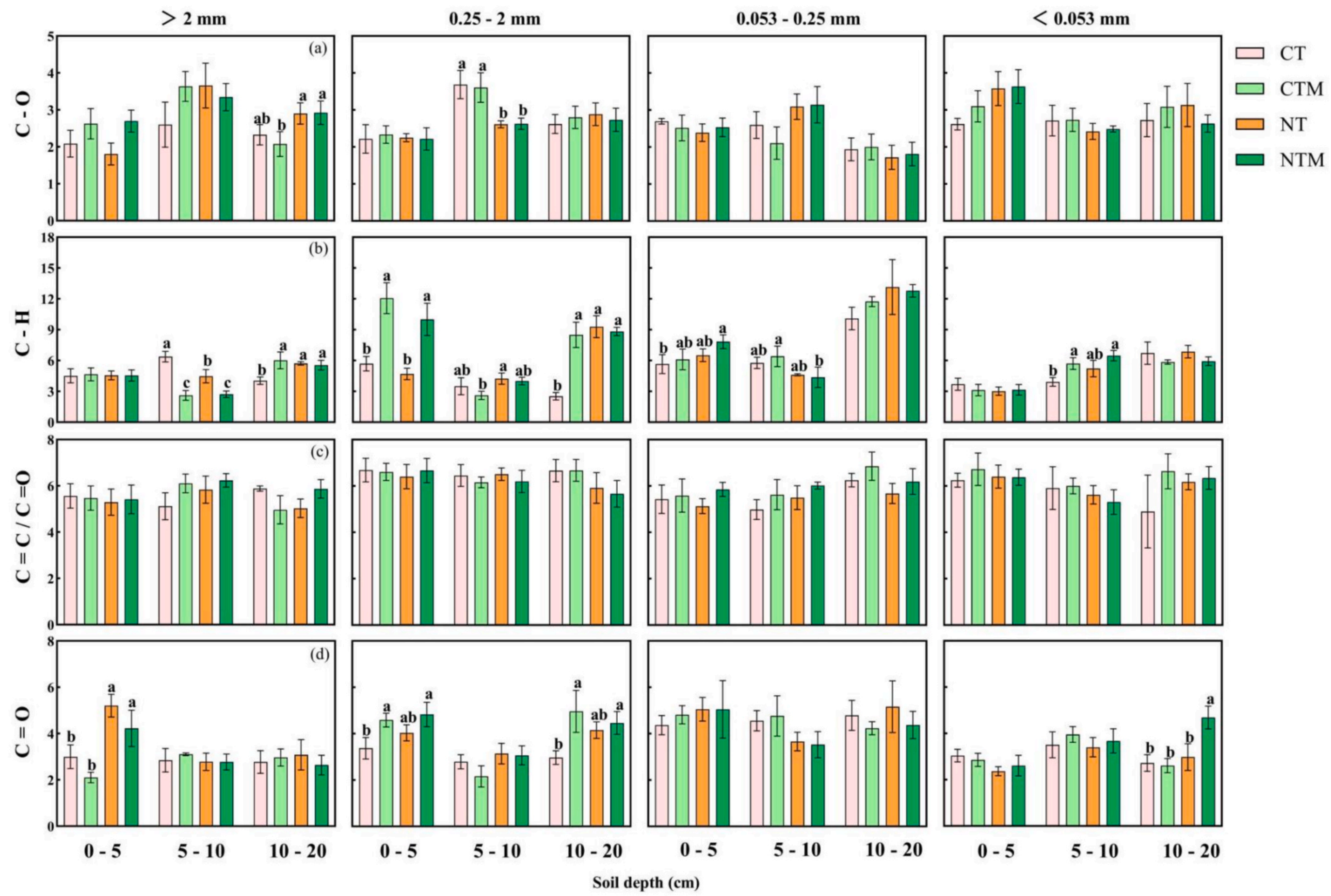

Fig. 4. Chemical composition of soil organic carbon in soil aggregates as influenced by conservation tillage practices, determined by FTIR spectroscopy. Results show the relative abundance of a) aliphatic carbon, b) polyol carbon, c) aromatic carbon, and d) carboxyl carbon within different aggregate size fractions across soil depths. Letters indicate significant differences between treatments at $p < 0.05$. CT: conventional tillage; CTM: conventional tillage-mulching; NT: no-tillage; NTM: no-tillage-mulching).

2.4. Soil physical and chemical analysis

2.4.1. Soil aggregate fractionation

Soil aggregates were separated using a dry sieving method (Tian et al., 2022). Pre-treated air-dried samples were passed through an 8 mm sieve, and 400 g of soil was placed in an automatic dry sieve shaker (Analysette3, Germany) with sieves of 2 mm, 0.25 mm, and 0.053 mm for 3 min. This yielded four aggregate size fractions: large macroaggregates (> 2 mm, LM), small macroaggregates (0.25 – 2 mm, SM), microaggregates (0.053 – 0.25 mm, MIC), and silt + clay (< 0.053 mm, SC) (Kan et al., 2020). The soil aggregate distribution (%) was expressed as the ratio of each aggregate fraction mass to the total soil mass. Soil aggregate stability indices, including mean weight diameter (MWD) and geometric mean diameter (GMD), were calculated using the following formulas (Li et al., 2024; Cheng et al., 2023):

$$MWD = \frac{\sum_{i=1}^{n}(X_i W_i)}{\sum_{i=1}^{n} W_i} \tag{1}$$

$$GMD = exp\left(\frac{\sum_{i=1}^{n} W_i lnX_i}{\sum_{i=1}^{n} W_i}\right) \tag{2}$$

where X_i represents the mean diameter (mm) of each size fraction, and W_i represents the weight proportion of each size fraction.

2.4.2. Soil organic carbon and labile organic carbon measurement

SOC was measured using an elemental analyzer (FlashEA 1112, Thermo Finnigan). Easily oxidizable organic C was determined using the 333 mmol L^{-1} potassium permanganate oxidation method (Blair et al., 1995). Recalcitrant organic C (RDOC) (Blair et al., 1995) was calculated by subtracting EOC from SOC as:

$$RDOC = SOC - EOC \tag{3}$$

2.4.3. Soil aggregate chemical composition

Fourier transform infrared (FTIR) spectroscopy (Nicolet 6700) was used to assess the spectral characteristics of SOC in aggregate size classes. A sample of 2 mg of aggregate material was mixed uniformly with 200 mg of potassium bromide (KBr) in an agate mortar and ground thoroughly. The mixture was then pressed into pellets using a tablet press. The FTIR spectra were recorded in the range of 400 – 4000 cm^{-1} with a resolution of 4 cm^{-1}, scanning 32 times, and using pure KBr as the background for correction.

Samples were analyzed with Omnic8.2 software for baseline correction and smoothing, and peak areas were integrated using Origin2019 software. The relative peak area of functional groups was assessed, including aliphatic C–H (3000 – 2800 cm^{-1}), polysaccharide C-O (1170 – 1148 cm^{-1}), aromatic C=O/C=C (1650 – 1600 cm^{-1}), and carboxyl C=O (1740 – 1700 cm^{-1}). Labile C fractions, such as aliphatic-C and polysaccharides, were distinguished from stable fractions, such as aromatic- and carboxyl-C (Shao et al., 2019).

2.4.4. Soil enzyme activity

Six enzymes were analyzed using standardized colorimetric assays:

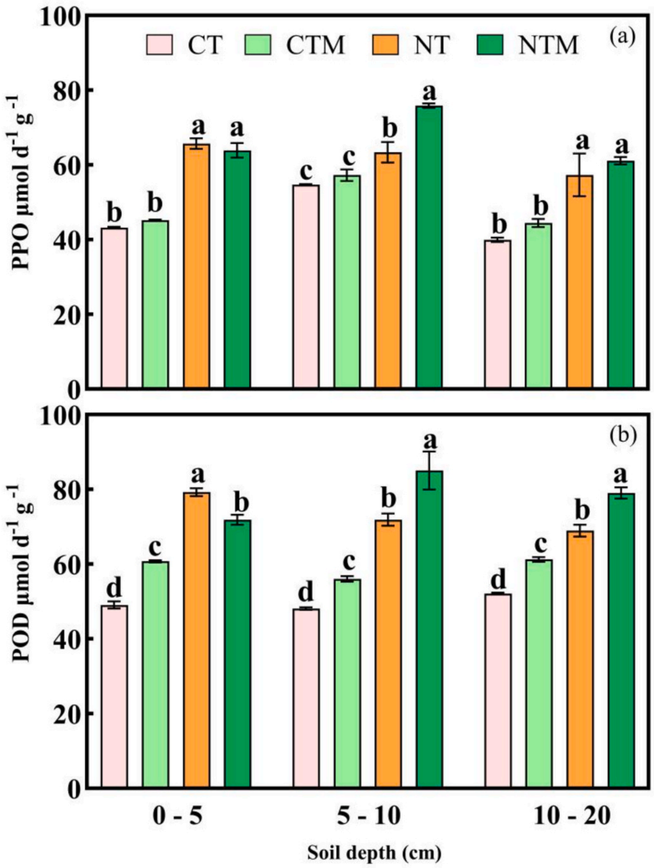

Fig. 5. Activities of oxidative enzymes (polyphenol oxidase, PPO; and peroxidase, POD) in response to different conservation tillage practices across soil depths. Values are expressed as enzyme units per gram of dry soil. Letters indicate significant differences between treatments at $p < 0.05$. CT: conventional tillage; CTM: conventional tillage-mulching; NT: no-tillage; NTM: no-tillage-mulching).

β-1,4-glucosidase (BG), polyphenol oxidase (PPO), peroxidase (POD), β-1,4-xylosidase (BXYL), cellobiohydrolase (CBH), and chitinase (NAG).

For BG, BXYL, CBH, and NAG analyses, soil samples (0.1 g) were suspended in 1 mL of modified universal buffer (MUB, pH 6.0) and homogenized. Aliquots (100 μL) of the soil suspension were transferred to microcentrifuge tubes and combined with 100 μL of 4-methylumbelliferyl (MUF)-linked substrate solution specific to each enzyme. The reaction mixtures were incubated at 30 °C with continuous agitation (180 rpm) in darkness for 3 h. Following incubation, aliquots (134 μL) were transferred to opaque microplate wells and combined with 66 μL of 0.5 M sodium hydroxide solution to terminate the reaction. Fluorometric measurements were conducted at $\lambda_{ex} = 365$ nm and $\lambda_{em} = 470$ nm. Enzyme activities (U) were calculated as:

$$U = (\Delta A + 2266.4)/62629 \times V/T/W \quad (4)$$

where V represents the extraction volume (1 mL), W denotes soil mass (g), and T indicates the reaction duration (3 h).

PPO and POD activities were determined using a micro-method approach (German et al., 2011; Tian et al., 2024). For PPO analysis, soil samples (0.02 g) were incubated with 120 μL of pyrogallol solution (50 mM) at 30 °C for 1 h, followed by sequential addition of 50 μL citrate–phosphate buffer (pH 6.0) and 430 μL diethyl ether. After multiple inversions and 30 min equilibration at room temperature, the absorbance of the supernatant (200 μL) was measured spectrophotometrically at 430 nm. POD analysis involved incubating soil samples (0.02 g) with 100 μL pyrogallol solution (50 mM) and 20 μL hydrogen peroxide (30 %) at 30 °C for 1 h, followed by addition of 50 μL citrate–phosphate buffer (pH 6.0) and 430 μL diethyl ether. Enzyme activities were calculated as:

$$U = (A + 0.003)/4.485 \times Vtotal/W/T \quad (5)$$

where V_{total} represents the total reaction volume (0.6 mL), T denotes reaction time (1 h), and W indicates soil mass.

2.5. Statistical analyses

Treatment effects were evaluated using analysis of variance (ANOVA) with significance determined at p < 0.05. Correlation heatmaps were generated to visualize relationships between organic C fractions and physical, chemical, and biological indicators across treatments. The relationships between soil physicochemical properties, biological enzyme activities, and organic C fractions in the 0—10 cm horizon under conservation tillage practices were evaluated using Mantel tests and Spearman correlation analyses, implemented through the "ggcor" package in R 4.2.2. Structural equation modeling (SEM) was employed to evaluate the impacts of no-tillage and mulching practices on organic C dynamics. Initial variable selection was informed by principal component analysis (PCA) and Pearson correlations. Indicators were categorized into physical, chemical, and biological parameters. After indicator screening, the model framework was constructed using the "piecewiseSEM" package in R 4.2.2. Model fit was assessed using the chi-square test ($\chi 2 = 11.03$, df = 7, p = 0.14) and the ratio of chi-square to degrees of freedom (CMIN/DF). All statistical analyses were performed using SPSS version 22. Graphical representations were generated using SigmaPlot 15.0.

3. Results

3.1. Soil aggregate distribution and stability

Across all treatments, large macroaggregates dominated in the soil composition (Fig. 1). In the 0—5 cm, conventional tillage-mulching, no-tillage, and no-tillage-mulching increased the proportion of macroaggregates compared to CT ($p < 0.05$). No-tillage-mulching reduced the proportion of 0.25 – 2 mm aggregates, while microaggregates ($p < 0.05$) and silt + clay (< 0.053 mm) fractions remained unchanged. In the 5 – 10 cm, conventional tillage-mulching, no-tillage, and no-tillage-mulching reduced the proportion of silt + clay ($p < 0.05$), whereas no differences were observed at 10 – 20 cm. Conventional tillage-mulching, no-tillage, and no-tillage-mulching enhanced MWD in the 0 – 5 cm compared to CT (Fig. 2, $p < 0.05$); conventional tillage-mulching increased GMD in the 0 – 5 cm ($p < 0.05$). Tillage and mulching did not affect MWD or GMD in 5 – 20 cm.

3.2. Distribution of SOC across aggregate sizes under conservation tillage

No-tillage-mulching enhanced SOC accumulation the most across aggregate fractions (Fig. 3). Conventional tillage-mulching showed no differences in SOC or its fractions across aggregate sizes compared to CT. No-tillage-mulching increased SOC, EOC, and RDOC contents throughout the 0 – 30 cm in large macroaggregates. In small macroaggregates, no-tillage-mulching enhanced SOC and EOC contents in the 0 – 20 cm, with additional increases in RDOC observed in the 0 – 5 cm and 10 – 20 cm (Fig. 3a–c).

In larger aggregates (> 2 mm and 0.25 – 2 mm), no-tillage increased SOC content in the 0 – 5 cm, EOC in the 10 – 20 cm, and RDOC in the 0 – 10 cm for > 2 mm aggregates. Within small macroaggregates, no-tillage enhanced SOC, EOC, and RDOC contents in the 0 – 5 cm, and increased SOC and EOC in the 10 – 20 cm (Fig. 3a–c, p < 0.05).

For small aggregates (0.053 – 0.25 mm and < 0.053 mm), no-tillage increased SOC, EOC, and RDOC contents in the 0 – 5 cm ($p < 0.05$). No-tillage-mulching increased SOC and RDOC throughout the 0 – 30 cm,

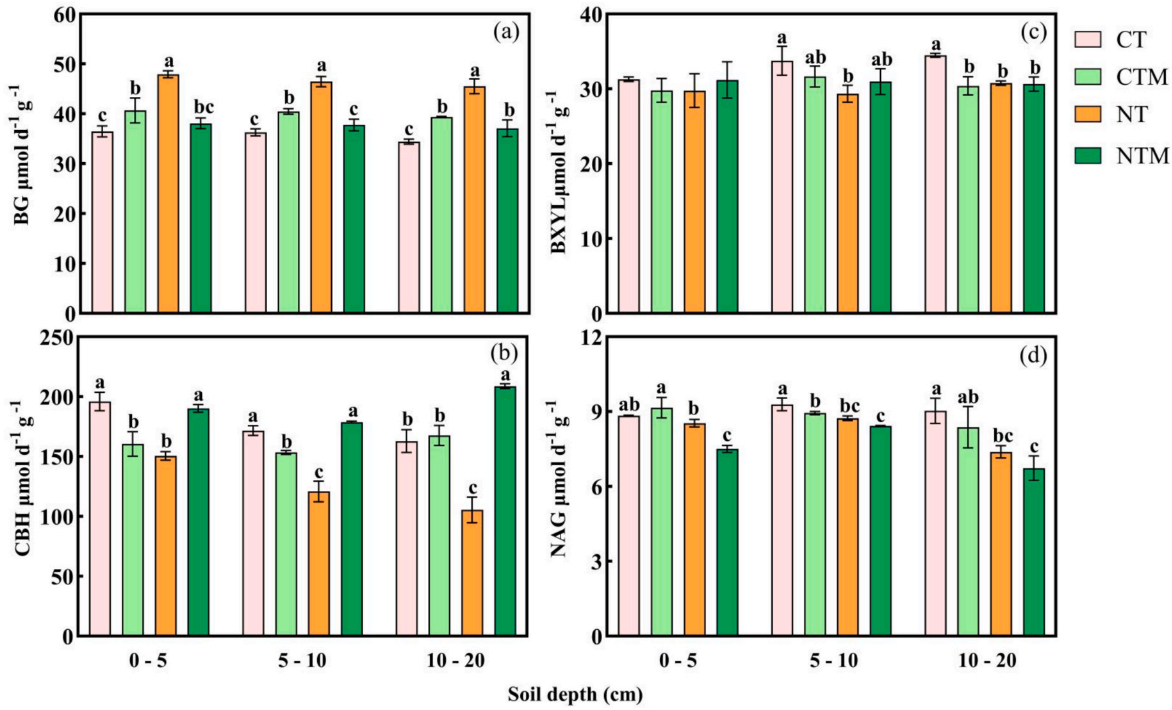

Fig. 6. Effects of conservation tillage practices on hydrolytic enzyme activities (β-glucosidase, BG; *β*-xylosidase, BXYL; cellobiohydrolase, CBH; and N-acetyl-*β*-glucosaminidase, NAG) at different soil depths. Values are expressed as enzyme units per gram of dry soil. Letters indicate significant differences between treatments at $p < 0.05$. CT: conventional tillage; CTM: conventional tillage-mulching; NT: no-tillage; NTM: no-tillage-mulching).

with EOC increases in the 0 – 5 cm and 10 – 20 cm ($p < 0.05$). In < 0.053 mm aggregates, no-tillage-mulching enhanced SOC and EOC in the 0 – 5 cm and 10 – 20 cm (Fig. 3a–c, $p < 0.05$).

3.3. *Changes in SOC chemical composition in soil aggregates under conservation tillage*

Conventional tillage-mulching, no-tillage, and (Fig. 3a–c, $p < 0.05$) no-tillage-mulching influenced the chemical composition of labile SOC fractions across all aggregate sizes, particularly affecting aliphatic-C content. Effects were most pronounced in larger aggregates (>2 mm and 0.25 – 2 mm) for polysaccharide-C and carboxyl-C in the stable SOC fraction (Fig. 4).

Conventional tillage-mulching reduced aliphatic C content within large macroaggregates in the 5 – 10 cm ($p < 0.05$), while increased aliphatic-C across multiple fractions: small macroaggregates at 0 – 5 cm, < 0.053 mm aggregates at 5 – 10 cm, and large aggregates (> 2 mm and 0.25 – 2 mm) in the 10 – 20 cm (Figs. 4a, b).

No-tillage decreased in aliphatic-C content within both 0.25 – 2 mm and > 2 mm aggregates in the 5 – 10 cm, coupled with increases in these same fractions at 10 – 20 cm. No-tillage-mulching influenced polysaccharide-C (0.25 – 2 mm) and aliphatic-C (> 2 mm) at 5 – 10 cm, while increased aliphatic-C across multiple fractions: 0.25 – 2 mm and 0.053 – 2 mm in the 0 – 5 cm, < 0.053 mm in the 5 – 10 cm, and both > 2 mm and 0.25 – 2 mm in the 10 – 20 cm (Fig. 4 ab).

Within the stable SOC fraction, while aromatic-C content remained unchanged across all treatments in > 2 mm and 0.25 – 2 mm aggregates, carboxyl-C showed treatment-specific responses. Conventional tillage-mulching enhanced carboxyl-C content in 0.25 – 2 mm aggregates at 0 – 5 cm and 10 – 20 cm ($p < 0.05$). No-tillage increased carboxyl-C in > 2 mm aggregates at 0 – 5 cm. No-tillage-mulching increased carboxyl-C in > 2 mm and 0.25 – 2 mm aggregates in the 0 – 5 cm, and in 0.25 – 2 mm and < 0.053 mm aggregates in the 10 – 20 cm (Figs. 4c, d, $p < 0.05$).

3.4. *Soil enzyme activities under different tillage treatments*

The conventional tillage-mulching increased POD activity in the 0 – 30 cm soil compared to CT (Fig. 5, $p < 0.05$). No-tillage and no-tillage-mulching increased PPO and POD activities in the 0 – 30 cm soil (Figs. 5a, b). In soil hydrolases, conservation tillage practices (conventional tillage-mulching, no-tillage and no-tillage-mulching) increased BG activity while reducing NAG and BXYL activities. The conventional tillage-mulching and no-tillage decreased CBH activity, whereas the no-tillage-mulching increased CBH activity (Fig. 6). The conventional tillage-mulching increased BG activity in the 0 – 30 cm compared to CT, but decreased CBH activity in the 0 – 10 cm, NAG activity in the 5 – 10 cm, and BXYL activity in the 10 – 20 cm ($p < 0.05$). No-tillage increased BG activity in the 0 – 30 cm and decreased CBH activity in the 0 – 20 cm and BXYL and NAG activities in the 10 – 20 cm ($p < 0.05$). No-tillage-mulching increased BG activity in the 10 – 20 cm, while decreasing NAG activity in the 0 – 20 cm and BXYL activity in the 10 – 20 cm ($p < 0.05$).

3.5. *Mechanisms improving SOC content and stability under conservation tillage*

Large macroaggregates decreased with small macroaggregates, microaggregates, aromatic-C content in small macroaggregates, and POD and CBH enzyme activities (Fig. 7). Positive correlations were observed with MWD, GMD, aliphatic-C content in large macroaggregates, and PPO, BXYL, and NAG enzyme activities.

The structural equation modeling showed, that no-tillage increased activities of soil enzyme (Fig. 8, path coefficient = 0.77, $p < 0.001$). Mulching practices showed positive associations with soil aggregation (0.60, $p < 0.01$) and enzyme activities (0.32, $p < 0.05$). Chemical composition demonstrated a positive relationship with EOC (0.74, $p < 0.001$). Multiple pathways influenced RDOC content, with positive relationships observed from soil aggregation (0.21, $p < 0.05$), enzyme activities (0.52, $p < 0.001$), and EOC (0.51, $p < 0.01$). Total SOC content

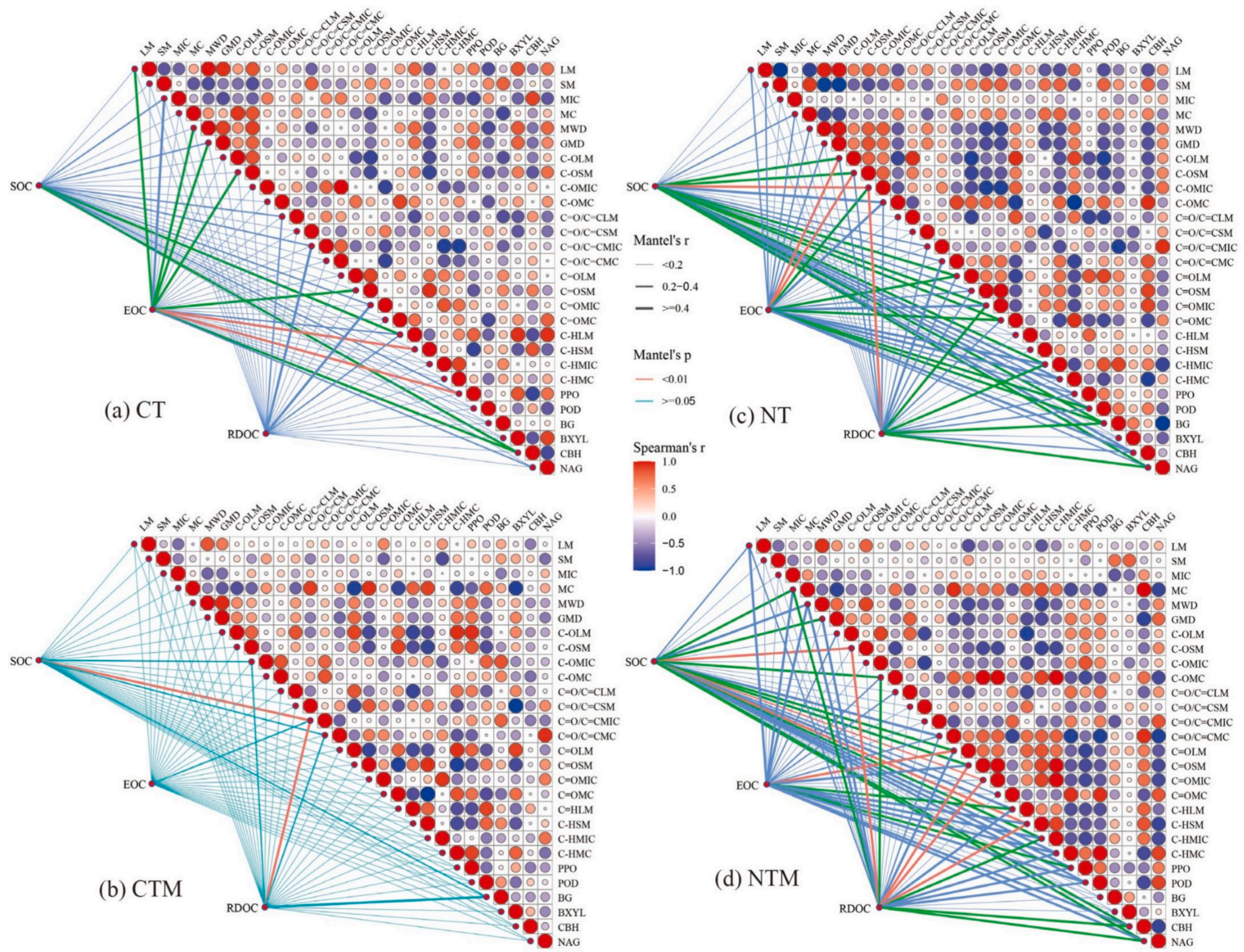

Fig. 7. Relationships between soil physicochemical properties, biological enzyme activities, and organic carbon fractions in the 0–10 cm soil under a) conventional tillage (CT), b) conventional tillage-mulching (CTM), c) no-tillage (NT), and d) no-tillage-mulching (NTM). Abbreviations: SOC, total soil organic carbon; EOC, easily oxidizable organic carbon; RDOC, recalcitrant dissolved organic carbon; LM, soil aggregates > 2 mm; SM, soil aggregates 0.25–2 mm; MIC, soil aggregates 0.053–0.25 mm; MC, soil aggregates < 0.053 mm; MWD, mean weight diameter of soil aggregates; GMD, geometric mean diameter of soil aggregates; C-OLM, polyol carbon in > 2 mm aggregates; C-OSM, polyol carbon in 0.25–2 mm aggregates; C-OMIC, polyol carbon in 0.053–0.25 mm aggregates; C-OMC, polyol carbon in < 0.053 mm aggregates; C=O/C=CLM, aromatic carbon in > 2 mm aggregates; C=O/C=CSM, aromatic carbon in 0.25–2 mm aggregates; C=O/C=CMIC, aromatic carbon in 0.053–0.25 mm aggregates; C=O/C=CMC, aromatic carbon in < 0.053 mm aggregates; C=OLM, carbonyl carbon in > 2 mm aggregates; C=OSM, carbonyl carbon in 0.25–2 mm aggregates; C=OMIC, carbonyl carbon in 0.053–0.25 mm aggregates; C=OMC, carbonyl carbon in < 0.053 mm aggregates; C-HLM, aliphatic carbon in > 2 mm aggregates; C-HSM, aliphatic carbon in 0.25–2 mm aggregates; C-HMIC, aliphatic carbon in 0.053–0.25 mm aggregates; C-HMC, aliphatic carbon in < 0.053 mm aggregates; PPO, polyphenol oxidase; POD, peroxidase; BG, β-1,4-glucosidase; BXYL, *β*-1,4-xylosidase; CBH, cellobiohydrolase; NAG, *β*-N-acetylglucosaminidase.

was positively influenced by enzyme activities (0.51, $p < 0.001$) and EOC (0.50, $p < 0.001$).

4. Discussion

4.1. Physical mechanisms of SOC stabilization

No-tillage-mulching increased macroaggregates (> 2 mm) at the 0 – 5 cm compared to conventional tillage. This result aligns with the first hypothesis and is consistent with other studies, which indicate that minimizing soil disturbance and supplying surface residues can strengthen aggregate stability (Six et al., 2002; Xiao et al., 2024). Macroaggregates physically encapsulate SOC, thereby reducing its susceptibility to microbial decomposition and erosion (Bronick and Lal, 2005; Debasish-Saha et al., 2012). In Karst ecosystems, characterized by shallow soil depths, high infiltration rates, and frequent erosive rainfall (Liu et al., 2024; Qin et al., 2017), the stability of macroaggregates is crucial for mitigating SOC losses and preserving soil fertility. Even if no-tillage alone reduces mechanical disruption, residue mulching appears to be essential for sustaining new aggregate formation and offsetting potential drawbacks of low soil aeration associated with no-tillage (Rocco et al., 2024). The mulching provides additional organic substrates (e.g., polysaccharides, root exudates) that stimulate microbial activity (Van et al., 2023). The secretions of soil microorganisms, including exopolysaccharides, facilitate the aggregation of micro-aggregates into macroaggregates (Acharya et al., 2024; Sainju et al., 2003). Consequently, combining no-tillage-mulching produces a synergistic effect that enhances soil structure and SOC protection more effectively than either practice alone.

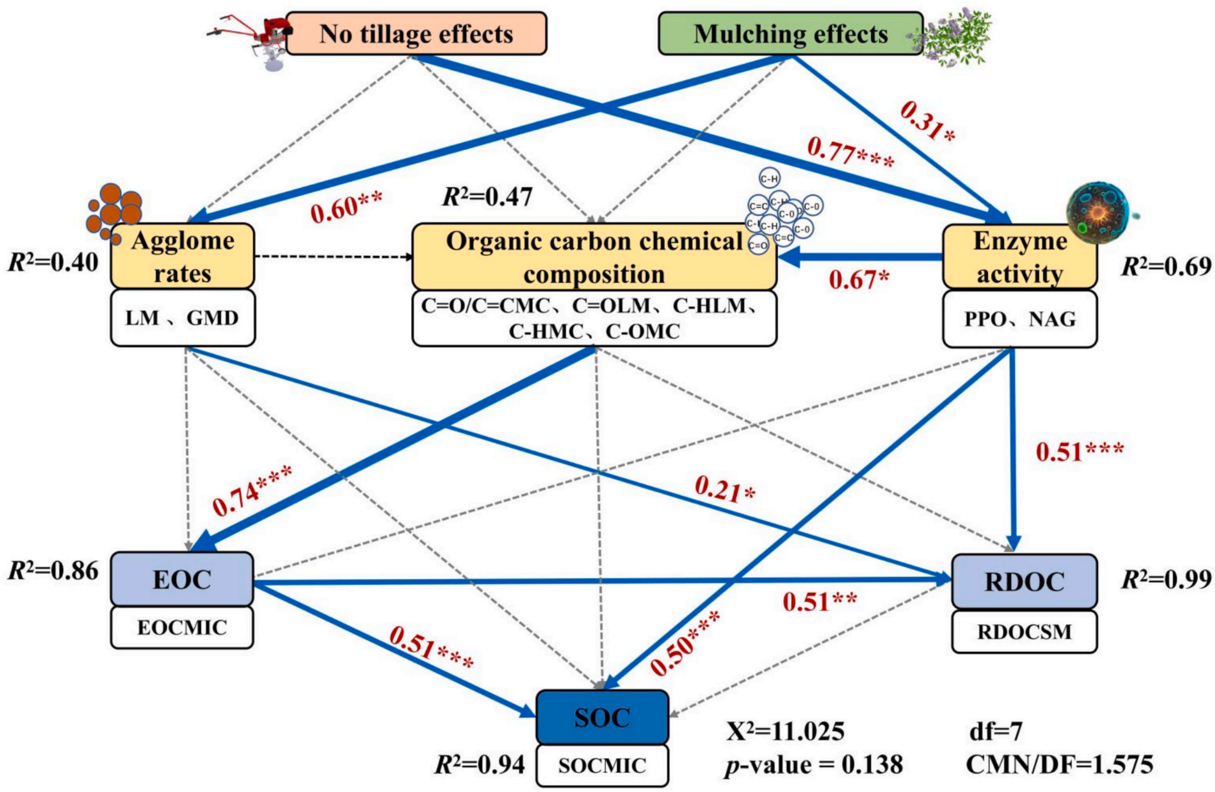

Fig. 8. Structural equation modeling (SEM) analysis examining the effects of soil physical structure (aggregate distribution and stability), chemical properties (organic carbon chemical composition), and biological enzyme activities (oxidases and hydrolases) on organic carbon fractions (SOC, EOC, and RDOC) under conservation tillage practices. Solid black arrows indicate significant relationships ($p < 0.05$), while dashed arrows represent non-significant pathways ($p > 0.05$). Variables included in the model (represented by boxes) are: LM, soil aggregates > 2 mm; GMD, geometric mean diameter of soil aggregates; C=O/C=CMC, aromatic carbon in < 0.053 mm aggregates; C=OLM, carbonyl carbon in > 2 mm aggregates; C-HLM, aliphatic carbon in > 2 mm aggregates; C-HMC, aliphatic carbon in < 0.053 mm aggregates; C-OMC, polyol carbon in < 0.053 mm aggregates; PPO, polyphenol oxidase; NAG, β-N-acetylglucosaminidase; EOCMIC, easily oxidizable organic carbon in 0.053–0.25 mm aggregates; RDOCSM, recalcitrant dissolved organic carbon in 0.25–2 mm aggregates; SOCMIC, soil organic carbon in 0.053–0.25 mm aggregates. Significance levels are denoted as: * $p < 0.05$, ** $p < 0.01$, *** $p < 0.001$. Model fit statistics: $\chi^2 = 11.03$, df = 7, $p = 0.14$, CMIN/DF = 1.58.

4.2. Chemical stabilization of SOC

FTIR spectroscopy indicated that no-tillage and no-tillage-mulching not only increased total SOC but also enriched recalcitrant fractions, such as carboxyl-C rich compounds. This finding supports the third hypothesis, suggesting that conservation tillage systems promote humification processes that convert labile organic inputs into more chemically stable forms (Leifeld and Kögel-Knabner, 2005. Kögel-Knabner, 2002; Lehmann and Kleber, 2015). These carboxyl-rich fractions resist microbial breakdown, thereby extending the residence time of SOC in soil (Poeplau and Don, 2013; Guggenberger et al., 2006). Although aromatic-C content showed no changes within three years, prolonged application of no-tillage or no-tillage-mulching may increase aromatic fractions in the long term as SOC matures and undergoes further humification (Shao et al., 2019).

Soils in Karst regions often contain high concentrations of calcium carbonate, potentially forming organo-mineral complexes that protect SOC (Lützow et al., 2006; Wasak and Drewnik, 2015; Qin et al., 2017; Hu et al., 2022). Thus, the accumulation of carboxyl and other high-energy SOC fractions may be facilitated by Ca^{2+}-mediated bridges or by ligand exchange with hydroxyl/carboxyl groups on humic substances (Hu and Lan, 2020). By combining residue mulching with minimal soil disturbance, no-tillage and no-tillage-mulching can optimize these organo-mineral associations, further reducing SOC turnover rates in soils in Karst regions. The present study primarily focused on changes in functional groups, whereas future work could delve deeper into how Ca^{2+} and associated mineral phases specifically reinforce chemical stabilization pathways in these soils.

4.3. Biological mediation of SOC stabilization

The fourth hypothesis proposed that no-tillage and no-tillage-mulching would improve soil enzyme activities associated with C cycling, including β-1,4-glucosidase and polyphenol oxidase. The results partly affirmed this hypothesis, though certain enzymes (e.g., peroxidase, cellobiohydrolase) demonstrated inverse correlations with macroaggregate formation. These mixed responses showed that even if macroaggregates protect SOC, they can also limit enzyme access to substrates (Allison and Jastrow, 2006; Six et al., 2002). Nevertheless, maintaining a favorable microhabitat under reduced disturbance and residue cover ensures that microbial populations continue to transform fresh organic inputs into more recalcitrant forms (Nannipieri et al., 2018). This simultaneous increase in physical protection and biological activity underscores a dynamic equilibrium: some enzymes are restricted from degrading more protected SOC, whereas others remain active enough to process newly added residues.

Karst conditions (e.g., shallow rooting zones, frequent rainfall events) amplify the importance of rapid yet stable C dynamics (Qin et al., 2017; Hu et al., 2022). Our findings indicate that active microbial communities and persistent enzyme production not only decompose fresh residues into simpler compounds but also promote aggregate binding via polysaccharide exudates (Burns et al., 2013). Over time, these transformations contribute to the formation of stable macroaggregates and the accumulation of recalcitrant C fractions, thereby establishing a reinforcing loop between soil structure and biological processes.

4.4. Integrating physical, chemical, and biological pathways affecting SOC

Based on SEM, no-tillage increased enzyme activities (path coefficient = 0.77), whereas mulching promoted macroaggregation (0.60) and enzyme activity (0.32). These improvements extended to EOC, which contributed to more stable fractions, including RDOC. In summarizing these relationships, three interconnected stabilization mechanisms emerge: (1) physical protection pathway, minimizing soil disturbance enhances macroaggregate stability, reducing erosion and limiting SOC exposure to decomposition (Post and Kwon, 2000; Six et al., 2002; Bronick and Lal, 2005); (2) chemical stabilization pathway, labile inputs are gradually converted to carboxyl- and aromatic-C rich fractions that resist decomposition. Mineral interactions in soils in Karst regions may further solidify this chemical stability (Kögel-Knabner, 2002; Lehmann and Kleber, 2015); (3) biological mediation pathway, microbial populations and enzymes transform plant residues into recalcitrant compounds and produce binding agents (Nannipieri et al., 2018). This sustains both SOC turnover and macroaggregate formation, reinforcing a stable soil architecture (Jastrow et al., 2007). These pathways operate in tandem, illustrating that effective SOC stabilization in Karst environments simultaneously depends on managing multiple soil processes.

4.5. Implications for Karst agroecosystem management

Given the shallow soils and intense erosion risks in Karst systems, simply reducing tillage may not be sufficient to preserve SOC and maintain fertility. The present findings highlight the need to integrate surface residue mulching with no-tillage to achieve robust aggregation, enrich recalcitrant SOC fractions, and maintain biologically active conditions. This approach aligns with other studies demonstrating that cover crop residues and minimal disturbance can enhance microbial biomass, improve nutrient cycling, and enhance overall soil health (Blanco-Canqui et al., 2015; Li et al., 2021).

These results have practical significance for mitigating soil degradation and enhancing C sequestration, particularly in ecologically sensitive Karst agroecosystems that suffer from frequent rainfall and nutrient leaching. By simultaneously optimizing physical protection, chemical stability, and biological activity, no-tillage-mulching offers a comprehensive strategy for enhancing soil resilience, reducing erosion, and potentially contributing to global climate change mitigation through increased SOC retention.

5. Conclusion

This study demonstrated that combining no-tillage with mulching offers multiple benefits for soil structure and C dynamics in Karst agroecosystems. First, no-tillage-mulching produced greater macroaggregate formation than either no-tillage or mulching alone, thereby enhancing physical protection of SOC. Second, the accumulation of carboxyl-C rich fractions under no-tillage-mulching indicated shifts toward more humified organic matter, supporting improved chemical stabilization of SOC. Third, conservation tillage influenced C dynamics via interconnected pathways encompassing physical aggregation, chemical composition, and microbial activity. Finally, elevated enzyme activities under no-tillage-mulching highlighted robust microbial responses that promoted C turnover and progressive stabilization. These findings highlight the value of conservation tillage strategies, especially no-tillage-mulching, for improving soil quality and sequestering organic C in fragile Karst ecosystems. By acknowledging the synergistic roles of physical, chemical, and biological processes, agricultural management in these environments can be optimized for both productivity and long-term ecological sustainability.

CRediT authorship contribution statement

Guang Xu: Writing – original draft, Visualization, Software, Investigation, Formal analysis, Data curation. **Qishun Mo:** Resources, Investigation, Data curation. **Zhou Li:** Writing – review & editing, Writing – original draft, Supervision, Resources, Project administration, Funding acquisition, Conceptualization. **Wangfei Qin:** Investigation, Data curation, Conceptualization. **Rui Dong:** Resources. **Xuechun Zhao:** Validation, Resources. **Chao Chen:** Funding acquisition. **Anna Gunina:** Writing – review & editing. **Narasinha Shurpali:** Writing – review & editing. **Tulasi Lakshmi Thentu:** Writing – review & editing. **Gang Nie:** Writing – review & editing. **Yuan Li:** Writing – review & editing, Writing – original draft, Methodology.

Declaration of competing interest

The authors declare that they have no known competing financial interests or personal relationships that could have appeared to influence the work reported in this paper.

Acknowledgments

This research was financed by the National Natural Science Foundation of China (32160337), the Guizhou Provincial Science and Technology Projects (Qian Ke He Zhi Cheng [2023] Yi Ban 473; QKHPTRC-CXTD [2022]011), and YL acknowledge the support from the AGCLIMATE project. We would like to acknowledge Shengjiang He (Farm Manager) for providing support for establishing and maintaining the research sites. We are grateful to Lihua Tian, Jie Pan, Shiyu Peng, Yinglai Shi, Junpeng Wei, Xiaowen Wang and Linye Jian for their contributions to the field data collection.

Appendix A. Supplementary data

Supplementary data to this article can be found online at https://doi.org/10.1016/j.catena.2025.109582.

References

Acharya, P., Ghimire, R., Idowu, O.J., Manoj, K., Shukla, M.K., 2024. Cover cropping enhanced soil aggregation and associated carbon and nitrogen storage in semi-arid silage cropping systems. Catena 245, 108264. https://doi.org/10.1016/j.catena.2024.108264.

Allison, S.D., Jastrow, J.D., 2006. Activities of extracellular enzymes in physically isolated fractions of restored grassland soils. Soil Boil Biochem. 38, 3245–3256. https://doi.org/10.1016/j.soilbio.2006.04.011.

Blair, G.J., Lefroy, R.D.B., Lisle, L., 1995. Soil carbon fractions based on their degree of oxidation, and the development of a carbon management index for agricultural systems. Aust. J. Agric. Res. 46, 1459–1466. https://doi.org/10.1071/AR9951459.

Blanco-Canqui, H., Shaver, T.M., Lindquist, J.L., Shapiro, C.A., Elmore, R.W., Francis, C. A., Hergert, G.W., 2015. Cover Crops and Ecosystem Services: Insights from Studies in Temperate Soils. Agron. J. 107, 2449–2474. https://doi.org/10.2134/agronj15.0086.

Bronick, C.J., Lal, R., 2005. Soil structure and management: a review. Geoderma 124, 3–22. https://doi.org/10.1016/j.geoderma.2004.03.005.

Burns, R.G., DeForest, J.L., Marxsen, J., Sinsabaugh, R.L., Stromberger, M.E., Wallenstein, M.D., Weintraub, M.N., Zoppini, A., 2013. Soil enzymes in a changing environment: current knowledge and future directions. Soil Boil Biochem. 58, 216–234. https://doi.org/10.1016/j.soilbio.2012.11.009.

Capriel, P., 1997. Hydrophobicity of organic matter in arable soils: influence of management. Eur. J. Soil Sci. 48, 457–462. https://doi.org/10.1111/j.1365-2389.1997.tb00211.x.

Cheng, Y.T., Xu, G.C., Wang, X.K., Li, P., Dang, X.H., Jiang, W.T., Ma, T.T., Wang, B., Gu, F.Y., Li, Z.B., 2023. Contribution of soil aggregate particle size to organic carbon and the effect of land use on its distribution in a typical small watershed on Loess Plateau, China. Ecol. Indic. 155, 110988. https://doi.org/10.1016/j.ecolind.2023.110988.

Debasish-Saha, S.S., Kukal, S.S., Bawa, S.S., 2012. Soil organic carbon stock and fractions in relation to land use and soil depth in the degraded Shiwaliks hills of lower Himalayas. Land Degrad. Dev. 25, 407–416. https://doi.org/10.1002/ldr.2151.

German, D.P., Weintraub, M.N., Grandy, A.S., Lauber, C.L., Rinkes, Z.L., Steven, D., Allison, S.D., 2011. Optimization of hydrolytic and oxidative enzyme methods for ecosystem studies. Soil Boil Biochem. 43, 1387–1397. https://doi.org/10.1016/j.soilbio.2011.03.017.

Guggenberger, G., Christensen, B.T., Zech, W., 2006. Land-use effects on the composition of organic matter in particle-size separates of soil: I. Lignin and carbohydrate signature. Eur. J. Soil Sci. 45, 449–458. https://doi.org/10.1111/j.1365-2389.1994.tb00530.x.

Hashimi, R., Huang, Q.L., Dewi, R.K., Nishiwaki, J.K., Komatsuzaki, M., 2023. No-tillage and rye cover crop systems improve soil water retention by increasing soil organic carbon in Andosols under humid subtropical climate. Soil Tillage Res. 234, 105861. https://doi.org/10.1016/j.still.2023.105861.

He, L.Y., Lu, S.X., Wang, C.G., Mu, J., Zhang, Y.L., Wang, X.D., 2021. Changes in soil organic carbon fractions and enzyme activities in response to tillage practices in the Loess Plateau of China. Soil Tillage Res. 209, 104940. https://doi.org/10.1016/j.still.2021.104940.

Honkanen, H., Turtola, E., Lemola, R., Heikkinen, J., Nuutinen, V., Uusitalo, R., Kaseva, J., Regina, K., 2021. Response of boreal clay soil properties and erosion to ten years of no-till management. Soil Tillage Res. 212, 105043. https://doi.org/10.1016/j.still.2021.105043.

Hu, N., Lan, J., 2020. Impact of vegetation restoration on soil organic carbon stocks and aggregates in a karst rocky desertification area in Southwest China. J Soils Sediments 20, 1264–1275. https://doi.org/10.1007/s11368-019-02532-y.

Hu, L., Li, Q., Yan, J., Liu, C., Zhong, J., 2022. Vegetation restoration facilitates belowground microbial network complexity and recalcitrant soil organic carbon storage in southwest China karst region. Sci. Total Environ. 820, 153137. https://doi.org/10.1007/s10584-006-9178-3.

IUSS Working Group WRB. 2022. World Reference Base for Soil Resources. International soil classification system for naming soils and creating legends for soil maps, 4th edition International Union of Soil Sciences (IUSS), Vienna, Austria. https://obrl-soil.github.io/wrbsoil2022.

Jastrow, J.D., Amonette, J.E., Bailey, V.L., 2007. Mechanisms controlling soil carbon turnover and their potential application for enhancing carbon sequestration. Clim. Change 80, 5–23. https://doi.org/10.1007/s10584-006-9178-3.

Jiang, Z.C., Lian, Y.Q., Qin, X.Q., 2014. Rocky desertification in Southwest China: Impacts, causes, and restoration. Earth Sci. Rev. 132, 1–12. https://doi.org/10.1016/j.earscirev.2014.01.005.

Kan, Z.R., Ma, S.T., Liu, Q.Y., Liu, B.Y., Virk, A.L., Qi, J.Y., Zhao, X., Lal, R., Zhang, H.L., 2020. Carbon sequestration and mineralization in soil aggregates under long-term conservation tillage in the North China Plain. Catena 188, 104428. https://doi.org/10.1016/j.catena.2019.104428.

Kögel-Knabner, I., 2002. The macromolecular organic composition of plant and microbial residues as inputs to soil organic matter. Soil Boil Biochem. 34, 139–162. https://doi.org/10.1016/S0038-0717(01)00158-4.

Lal, R., 2004. Soil carbon sequestration to mitigate climate change. Geoderma 123 (1–2), 1–22. https://doi.org/10.1016/j.geoderma.2004.01.032.

Lehmann, J., Kleber, M., 2015. The contentious nature of soil organic matter. Nature 528, 60–68. https://doi.org/10.1038/nature16069.

Leifeld, J., Kögel-Knabner, I., 2005. Soil organic matter fractions as early indicators for carbon stock changes under different land-use? Geoderma 124 (1–2), 143–155. https://doi.org/10.1016/j.geoderma.2004.04.009.

Li, Y., Li, Z., Cui, S., Liang, G.P., Zhang, Q.P., 2021. Microbial-derived carbon components are critical for enhancing soil organic carbon in no-tillage croplands: a global perspective. Soil Tillage Res. 205, 104758. https://doi.org/10.1016/j.still.2020.104758.

Li, Z.G., Fan, Y.S., Zhang, R.H., Chen, P., Jing, X.X., Lyu, C.H., Zhang, R.Q., Li, Y.F., Liu, Y., 2024. Synergistic impacts of Landscape, Soil, and environmental factors on the spatial distribution of soil aggregates stability in the Danjiangkou reservoir area. Catena 237, 107840. https://doi.org/10.1016/j.catena.2024.107840.

Liu, L.J., Zhu, Q.L., Wan, Y.X., Yang, R.Y., Mou, J.X., Li, Y.H., Meng, L., Zhu, T.B., Elrys, A.S., 2024. Afforestation improves soil organic carbon and total nitrogen stocks mainly through increasing> 2 mm aggregate fractions and stimulating carbon and nitrogen transformations within aggregates in subtropical karst region. Catena 243, 108220. https://doi.org/10.1016/j.catena.2024.108220.

Liu, X.T., Song, X.J., Li, S.P., Liang, G.P., Wu, X.P., 2023. Understanding how conservation tillage promotes soil carbon accumulation: Insights into extracellular enzyme activities and carbon flows between aggregate fractions. Sci. Total Environ. 897, 165408. https://doi.org/10.1016/j.scitotenv.2023.165408.

Lützow, M., Kögel-Knabner, I., Ekschmitt, K., Matzner, E., Guggenberger, G., Marschner, B., Flessa, H., 2006. Stabilization of organic matter in temperate soils: mechanisms and their relevance under different soil conditions–a review. Eur. J. Soil Sci. 57 (4), 426–445. https://doi.org/10.1111/j.1365-2389.2006.00809.

Ma, Y.Q., Yu, Y., Nan, S.Z., Chai, Y., Xu, W.Y., Qin, Y., Li, X.L., Bodner, G., 2024. Conversion of SIC to SOC enhances soil carbon sequestration and soil structural stability in alpine ecosystems of the Qinghai-Tibet Plateau. Soil Boil Biochem. 195, 109452. https://doi.org/10.1016/j.soilbio.2024.109452.

Melero, S., López-Garrido, R., Murillo, J.M., Moreno, F., 2009. Conservation tillage: Short- and long-term effects on soil carbon fractions and enzymatic activities under Mediterranean conditions. Soil Tillage Res. 104, 292–298. https://doi.org/10.1016/j.still.2009.04.001.

Mhlanga, B., Pellegrino, E., Thierfelder, C., Ercoli, L., 2022. Conservation agriculture practices drive maize yield by regulating soil nutrient availability, arbuscular mycorrhizas, and plant nutrient uptake. Field Crops Res. 277, 108403. https://doi.org/10.1016/j.fcr.2021.108403.

Nannipieri, P., Trasar-Cepeda, C., Dick, R.P., 2018. Soil enzyme activity: a brief history and biochemistry as a basis for appropriate interpretations and meta-analysis. Biol. Fertil. 54, 11–19. https://doi.org/10.1007/s00374-017-1245-6.

Nebbioso, A., Piccolo, A., 2012. Advances in humeomics: enhanced structural identification of humic molecules after size fractionation of a soil humic acid. Anal. Chim. Acta 720, 77–90. https://doi.org/10.1016/j.aca.2012.01.027.

Peltre, C., Gregorich, E.G., Bruun, S., Jensen, L.S., Magid, J., 2017. Repeated application of organic waste affects soil organic matter composition: evidence from thermal analysis, FTIR-PAS, amino sugars and lignin biomarkers. Soil Boil Biochem. 104, 117–127. https://doi.org/10.1016/j.soilbio.2016.10.016.

Poeplau, C., Don, A., 2013. Sensitivity of soil organic carbon stocks and fractions to different land-use changes across Europe. Geoderma 192, 189–201. https://doi.org/10.1016/j.geoderma.2012.08.003.

Post, W.M., Kwon, K.C., 2000. Soil carbon sequestration and land-use change: processes and potential. Glob. Chang. Biol. 6 (3), 317–327. https://doi.org/10.1046/j.1365-2486.2000.00308.x.

Qin, W.F., Zhao, X.C., Yang, F., Chen, J.H., Mo, Q.S., Cui, S., Chen, C., He, S.J., Li, Z., 2023. Impact of fertilization and grazing on soil N and enzyme activities in a karst pasture ecosystem. Geoderma 437, 116578. https://doi.org/10.1016/j.geoderma.2023.116578.

Qin, Y.B., Xin, Z.B., Wang, D.M., Xiao, Y.L., 2017. Soil organic carbon storage and its influencing factors in the riparian woodlands of a chinese karst area. Catena 153, 21–29. https://doi.org/10.1016/j.catena.2017.01.031.

Reynaert, S., Hose, T.D., Boeck, H.J.D., Laorden, D., Dult, L., Verbruggen, E., Nijs, I., 2024. Can permanent grassland soils with elevated organic carbon buffer negative effects of more persistent precipitation regimes on forage grass performance? Sci. Total Environ. 918, 170623. https://doi.org/10.1016/j.scitotenv.2024.170623.

Rocco, S., Munkholm, L.J., Jensen, J.L., 2024. Long-term soil quality and C stock effects of tillage and cover cropping in a conservation agriculture system. Soil Tillage Res. 241, 106129. https://doi.org/10.1016/j.still.2024.106129.

Sainju, U.M., Whitehead, W.F., Singh, B.P., 2003. Cover crops and nitrogen fertilization effects on soil aggregation and carbon and nitrogen pools. Can. J. Soil Sci. 83, 155–165. https://doi.org/10.4141/S02-056.

Shao, P.S., Liang, C., Rubert-Nason, K., Li, X.Z., Xie, H.T., Bao, X.L., 2019. Secondary successional forests undergo tightly-coupled changes in soil microbial community structure and soil organic matter. Soil Boil Biochem. 128, 56–65. https://doi.org/10.1016/j.soilbio.2018.10.004.

Singh, A.K., Singh, J.B., Singh, R., Kantwa, S.R., Jha, P.K., Ahamad, S., Singh, A., Ghosh, A., Prasad, M., Singh, S., 2023. Understanding soil carbon and phosphorus dynamics under grass-legume intercropping in a semi-arid region. Agronomy 13, 1692. https://doi.org/10.3390/agronomy13071692.

Six, J., Conant, R.T., Paul, E.A., Paustian, K., 2002. Stabilization mechanisms of soil organic matter: Implications for C-saturation of soils. Plant and Soil 241, 155–176. https://doi.org/10.1023/A:1016125726789.

Tian, Q., Yang, F., Wang, Z.H., Zhang, Q.Y., 2024. Variation of soil organic carbon components and enzyme activities during the ecological restoration in a temperate forest. Ecol. Eng. 201, 107192. https://doi.org/10.1016/j.ecoleng.2024.107192.

Tian, S.Y., Zhu, B.J., Yin, R., Wang, M.W., Jiang, Y.J., Zhang, C.Z., Li, D.M., Chen, X.Y., Kardol, P., Liu, M.Q., 2022. Organic fertilization promotes crop productivity through changes in soil aggregation. Soil Boil Biochem. 165, 108533. https://doi.org/10.1016/j.soilbio.2021.108533.

United States Department of Agriculture (USDA), 1999, Soil Taxonomy, second ed. English, Washington. https://www.nrcs.usda.gov/resources/guides-and-instructions/soil-taxonomy.

Van, E., Laura, L., Chahal, I., Peng, Y.J., Awrey, J.C., 2023. Influence of cover crops at the four spheres: a review of ecosystem services, potential barriers, and future directions for North America. Sci. Total Environ. 858, 159990. https://doi.org/10.1016/j.scitotenv.2022.159990.

Wasak, K., Drewnik, M., 2015. Land use effects on soil organic carbon sequestration in calcareous Leptosols in former pastureland – a case study from the Tatra Mountains (Poland). Solid Earth 6 (4), 1103–1115. https://doi.org/10.5194/se-6-1103-2015.

Xiao, Y., Zhou, M., Liu, X.B., Zhang, X.Y., Xiao, L.L., Liu, J., Cruse, R.M., 2024. Pore connectivity and anisotropy affect carbon mineralization via extracellular enzymes in> 2 mm aggregates under conservation tillage of Mollisols. Soil Tillage Res. 244, 106253. https://doi.org/10.1016/j.still.2024.106253.

Xing, S.K., Zhang, G.H., Wang, C.S., Zhang, N., Chen, S.Q., 2023. Effects of straw incorporation on soil erosion resistance along a land degradation gradient in the black soil region of China. Catena 231, 107365. https://doi.org/10.1016/j.catena.2023.107365.

Xiong, Y.J., Qiu, G.Y., Mo, D.K., Lin, L., Sun, H., Wang, Q.X., Zhao, S.H., Yin, J., 2008. Rocky desertification and its causes in karst areas: a case study in Yongshun County, Hunan Province, China. Environ. Geol. 57, 1481–1488. https://doi.org/10.1007/s00254-008-1425-7.

Zhang, Y., Xu, X., Li, Z., Liu, M., Xu, C., Zhang, R., Luo, W., 2019. Effects of vegetation restoration on soil quality in degraded karst landscapes of southwest China. Sci. Total Environ. 650, 2657–2665. https://doi.org/10.1016/j.scitotenv.2018.09.372.

Zhu, Y.P., Zhang, H.P., Wang, Q.Y., Zhu, W.D., Kang, Y.H., 2024. Soil extracellular enzyme activity linkage with soil organic carbon under conservation tillage: a global meta-analysis. Eur. J. Agron. 155, 127135. https://doi.org/10.1016/j.eja.2024.127135.